International Journal of Heat and Mass Transfer 62 (2013) 223–229

Contents lists available at SciVerse ScienceDirect

International Journal of Heat and Mass Transfer

journal homepage: www.elsevier.com/locate/ijhmt

Thermal characteristics of inclined plate impinged by underexpanded sonic jet

Jiwoon Song, Jang Woo Lee, Man Sun Yu, Sangwoo Shin, Beom Seok Kim, Hyung Hee Cho *

Department of Mechanical Engineering, Yonsei University, 50 Yonsei-ro, Seodaemun-gu, Seoul 120-749, Republic of Korea

ARTICLE INFO

Article history:
Received 15 November 2012
Received in revised form 21 February 2013
Accepted 26 February 2013
Available online 27 March 2013

Keywords:
Underexpanded sonic jet
Inclined impingement
Recovery factor
Energy separation
IR thermography

ABSTRACT

The impingement of an underexpanded jet onto a solid object can be found in engineering applications. Takeoff and landing of V/STOL aircraft, and launching systems on a spaceship for solid rocket motors are some examples related to this complex phenomenon. Because most of the dynamic energy is converted to thermal energy when a high-speed flow is decelerated in front of a protruded solid body, impingement of the high-speed flow produces a severe thermal load to the body surface as well as aerodynamic loads on it. In this experimental study, the thermal characteristics on an inclined plate impinged by an underexpanded sonic jet were investigated. The recovery factor was retained by infrared thermography while the pressure distribution was measured using pressure transducers. Experiments were performed for four different inclinations of impinged plate, ranging from 0° to 30°. In addition, the effect of nozzle-to-plate distance was studied. From the results, the axi-symmetric pattern of recovery factor on an impinged surface is broken and the low recovery factor zone shifts to the downward region as the inclination angle increases. In addition, the cooling effect is weakened overall as the inclination angle increases.

© 2013 Elsevier Ltd. All rights reserved.

1. Introduction

Jet impingement study is primarily applicable to rocket and guided-weapon systems. Because impingement jet is operated in state of high pressure and temperature, the thermal effect of jet impingement to the solid surface should be studied to improve the thermal design safety of rocket and jet engine system applications. In such applications, thermal defect conditions might arise due to high temperature and pressure exhaust gas impinging close target surfaces.

Extensive studies conducted by many researchers [1–23] have revealed some interesting and complex phenomena related to such jet impingement. Fox et al. [2,3] studied the effect of vortex for impinging jet on high subsonic and supersonic flow. The concept of 'total temperature separation' was introduced by his subsonic research [2]. The vortex rings entrap the particles near the jet exit and make periodic negative and positive pressure motion at the jet edge. From these motions, the jet has a minimum temperature near the edge and a maximum inside the jet. And also vortex entraps the particle entrained from the ambient outside of the jet. These particles are increasing the temperature and reaching the maximum value of near the center of the jet. From each entrapped particle due to vortical motion causes the change of cooling effect at the target plate depending on the distance of the plate and the nozzle. They showed that unsteady vortical structure affects significantly the wall temperature and heat transfer. Based on subsonic results, Fox et al. [3] conducted the experiment on supersonic and found the 'shock-induced total temperature separation' which is not shown in the subsonic. It is due to the interaction of the shock structure of the supersonic with vortical structures near the jet exhaust. For more study about supersonic impinging jet, complex shock structures and their interactions have been extensively studied by Gubanova [4], Kalghatgi [5], Ginzburg [6], and Carling [7] using optical methods such as a shadowgraph and the Schlieren method. By using the Schlieren pictures and surface pressure distributions, the researchers analyzed shock structures and pressure distributions for objects at different inclination angles. For impinging sonic jets, Goldstein et al. [8] presented the radial distribution of the recovery factor and the local heat transfer for an axisymmetric impinging jet with a certain nozzle-to-plate spacing. Lamont and Hunt [9] studied the effect of axisymmetric underexpanded jets impinging on an inclined flat surface as well as a perpendicular surface. Kim and Chang [10] performed a numerical simulation of a supersonic underexpanded jet, with a focus on pressure and density, and compared the results with those from Lamont's experiment. Eckert [11] carried out an experiment on jet impingement on a plate with Reynolds numbers

* Corresponding author. Tel.: +82 2 2123 2828; fax: +82 2 312 2159.
E-mail address: hhcho@yonsei.ac.kr (H.H. Cho).

0017-9310/$ - see front matter © 2013 Elsevier Ltd. All rights reserved.
http://dx.doi.org/10.1016/j.ijheatmasstransfer.2013.02.066

Nomenclature

C_p	specific heat at constant pressure, kJ/kg·K	r	recovery factor $\left(=\frac{T_{aw}-T_s}{T_0-T_s}=\frac{T_{aw}-T_s}{T_d}=1+\frac{T_{aw}-T_0}{u_j^2/2C_p}\right)$
D	nozzle exit diameter	T	temperature
P	pressure	T_0	total temperature
P_a	ambient pressure	T_{aw}	adiabatic wall temperature
P_e	nozzle exit pressure	T_s	static temperature
P_c	chamber pressure	T_d	dynamic temperature
P_0	total pressure	u_j	velocity of a jet at the nozzle exit
PR	under-expansion ratio, P_e/P_a		
R	radial distance from the center		

ranging from 61,000 to 124,000. The thermal characteristics can be explained by "energy separation". Han et al. [12,13] used numerical analysis to determine the location and magnitude of energy separation for various nozzle-to-plate distances and study the dominant effect of the vortex. The magnitude of the energy separation in the radial direction was measured experimentally with a free jet for the Reynolds numbers ranging from 80,000 to 160,000 by Seol and Goldstein [14]. On the other hand, with regard to heat transfer research, Dytle and Webb [15] measured the thermal characteristics of the normal jet impinged surface using an infrared (IR) camera that was placed very close to the plate to overcome the limitation of using a thermocouple. In addition to this study, Huang [16], Liu [17], Behnia [18] and Baughn [19] also reported the study of heat transfer for impinging jet. However they performed the test only in the case of normal impingement. In our group, the thermal characteristics of a plate for various nozzle-to-plate distances and pressure ratios are investigated by Kim et al. [20]. The recovery factors $\left(=\frac{T_{aw}-T_s}{T_0-T_s}\right)$ which are difference between adiabatic wall temperature and total temperature are obtained by experimental investigation carried out the axisymmetric, underexpanded, and sonic jet impinging on flat plate on underexpansion ratio ranges from 1.5 to 3.5 and the nozzle exit to the plate adjusted from 0.5 to 20.0 nozzle-exit diameters. The highest recovery factor was observed at the stagnation point varies from 0.35 to 1.25 for the underexpansion ratio of P_e/P_a = 3.5. Yu et al. [21] carried out the study of heat transfer on flat surface impinged by an underexpanded sonic jet. They reported the distribution of the heat transfer coefficient on the central impingement region due to the interaction between the sonic surface and recirculation flow. High heat transfer on a surface formed due to turbulence diffusion from the shear layers around the jet edge and the sonic surface into a jet core. Both studies were for normal impinging jets.

However, most previous investigations on underexpanded impinging jets have concentrated primarily on the basic aspects of the flow shock structure and the surface pressure distributions. A few studies have been conducted on the thermal characteristics of an inclined surface impinged by a jet; in particular, an experimental approach for analyzing the energy separation phenomenon is hardly to be found. In this study, the recovery factor distribution for an impinged surface has been retained experimentally when the impinged surface is inclined relative to the jet center line. In addition, the distributions of the surface pressure have been measured to understand the flow structure on a surface. The inclination angle and the nozzle-to-plate distance have been selected as the parameters of interest. The two-dimensional temperature distribution was measured using infrared thermography (IRT). The results obtained in this study will aid in understanding the complicated thermal characteristics of a surface impinged by an underexpanded jet.

2. Experimental apparatus and method

Fig. 1 shows the schematic diagram of the experimental apparatus [20] used for the present study. Experimental apparatus is composed of reciprocating high pressure compressor, air filter, storage tanks, regulators, air actuator ball valve, settling chamber and nozzle. Air was compressed up to 150 kgf/cm^2 by a compressor and then passed through a cooling chamber. Moisture and oil is removed at five-stage filter. Then, it was reserved in storage tanks of which total storage capacity was 0.45 m^3. The compressed air was supplied to the settling chamber through pressure regulators (Yamato Sangyo, YR-5062) from the storage tanks. The nozzle, from which a jet issues, was mounted behind of the settling chamber. During the test, compressed air in the storage tanks was depressurized to the designed pressure level by the regulator and stagnated in the settling chamber to ensure flow uniformity and easy measurement of the stagnation pressure and temperature. Finally, the compressed air was accelerated through the convergent nozzle and injected into the atmosphere. The nozzle exit diameter

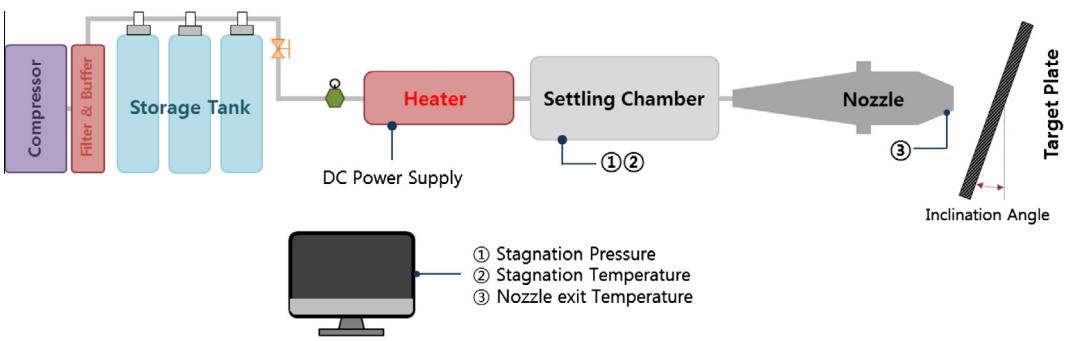

Fig. 1. Schematic of experimental apparatus.

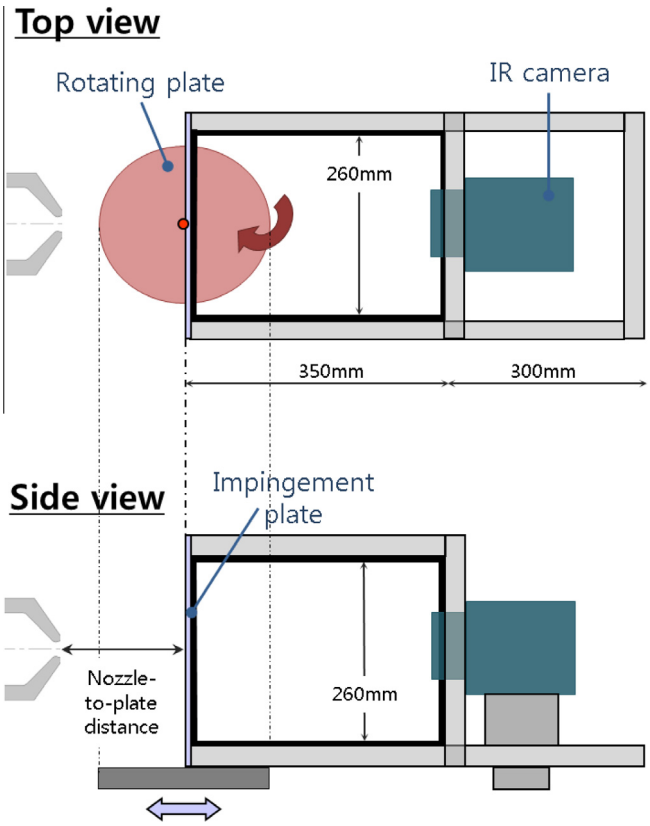

Fig. 2. Experimental setup with IR camera.

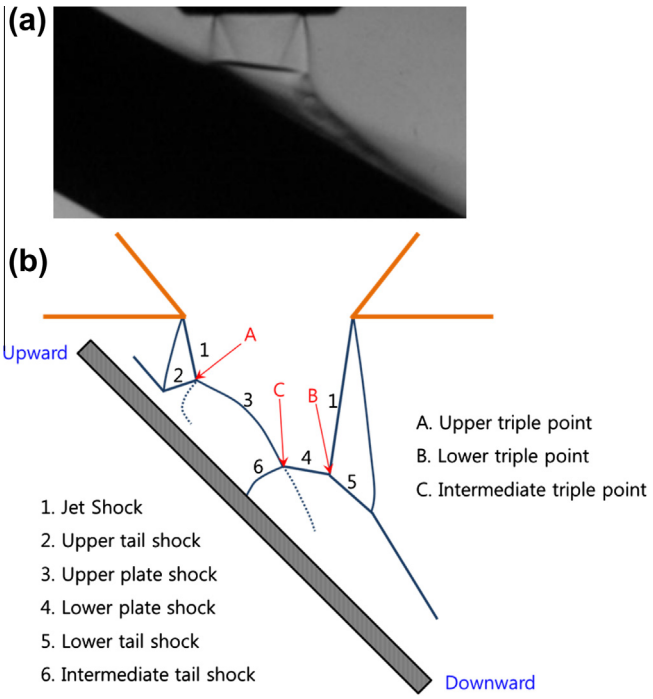

Fig. 3. (a) Shadowgraphs of impinging jets for $M_D = 1.0$, $P_e/P_a = 2.0$ and $Z_P/D = 1.0$, (b) Diagram of impinging jets of the shock configuration for underexpanded jet interaction with a inclined plate.

(=D) was 10 mm. In the case of the temperature measurement test, the constant stagnation temperature is an important factor. However, the gas stagnation temperature decreased naturally due to the isentropic expansion process in storage tanks and the Joule–Thomson effect, etc. To avoid this problem, the supplied air was heated with an electric heater installed between the storage tanks and settling chamber. In this study, the gas stagnation temperature was maintained at close to the ambient air temperature, within ±0.5 K, and minimizes the effect of entrainment of the ambient air.

Infrared thermography (IRT) was used to measure the two-dimensional adiabatic wall temperature distributions. Fig. 2 shows the IRT setup in this study. To measure the surface temperature without disturbing the jet flow, an IR camera was set at the opposite side of the impinged surface and the thermal image on the face was taken and stored in a computer. The impinged plate was a 260 × 260 mm and 0.7 mm thick piece of stainless steel. The thickness was chosen as a value to minimize surface deformation due to the high pressure on the jet impinged surface and provide a similar temperature level on both faces. To analyze the difference between both surfaces due to natural convection and radial direction heat dissipation, numerical and analytical calculations found the maximum temperature difference ratio and deformation angle of the plate to be 0.12% and 0.22°, respectively. The space between the opposite face and the IR camera was isolated from the external air by an acrylic box with insulation and the inner face of the box was coated with a black paint to minimize error due to the reflection and transmission of infrared rays. This measurement method was verified in the study of Shin et al. [22] by comparison with the results from thermocouple measurement.

Another test plate with two pressure taps in the central portion was used to measure the surface pressure. Each hole on the impinged surface was 0.8 mm in diameter, and the pressure tap was connected with a pressure transducer on the opposite side. The two pressure taps were spaced 20.0 mm apart. Detailed local distribution of pressure has been obtained by moving the pressure tap attached with an automatic moving system. Then the high-resolution data were obtained with spacing of 1 mm.

During the test, the underexpansion ratio was fixed to 1.5 and the inclination angle ranged from 0° to 30°. The effect of the location that the jet is applied to the impinged surface was also considered and the nozzle-to-plate distance was varied from 1D to 10D. Measured adiabatic wall temperature (T_{aw}) was converted to the recovery factor, and the relation is as follows:

$$r = \frac{T_{aw} - T_s}{T_0 - T_s} = \frac{T_{aw} - T_s}{T_d} = 1 + \frac{T_{aw} - T_0}{u_j^2/2C_p} \quad (1)$$

where T_0, T_s, T_d, and u_j are the total, static and dynamic temperatures and the average jet velocity at the nozzle exit plane, respectively.

3. Results and discussions

Fig. 3 shows shadowgraph results [23] and schematic of inclined jet impingement [9]. Very complex shock wave structure appears depending on the slope. These complex shock structure and intensity distributions change dramatically pressure and temperature on the impinged surface and affect wall jet region. Fig. 4 shows surface pressure distributions on a symmetric line of an impinged surface for various surface inclination angles. In this case, the nozzle-to-plate distance and pressure ratio were fixed at 1D and 1.5, respectively. The horizontal axis shows the non-dimensional radial position normalized by nozzle exit diameter (D) and the vertical axis shows the non-dimensional surface pressure normalized by the chamber pressure (P_c). In the radial position, a surface geometrical center is zero and the upward positions have the minus sign and vice versa. In all cases, due to a plate shock in front of the impinged surface, the maximum surface pressure is smaller than the chamber pressure, that is, P/P_c is smaller than 1.0. As the inclina-

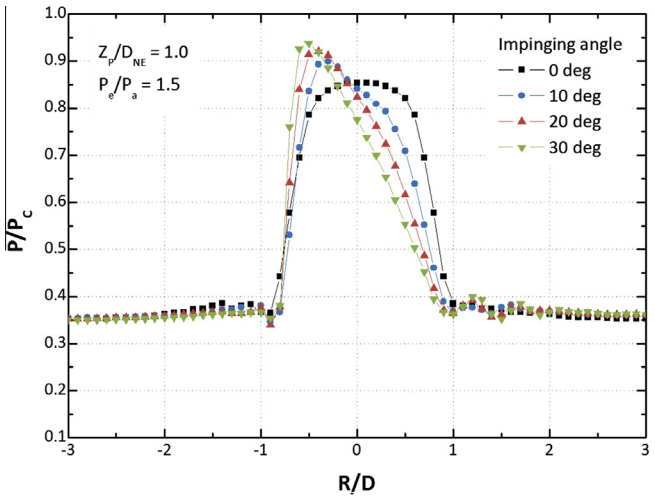

Fig. 4. Surface pressure distributions for various impinging angles at $Z/D = 1$.

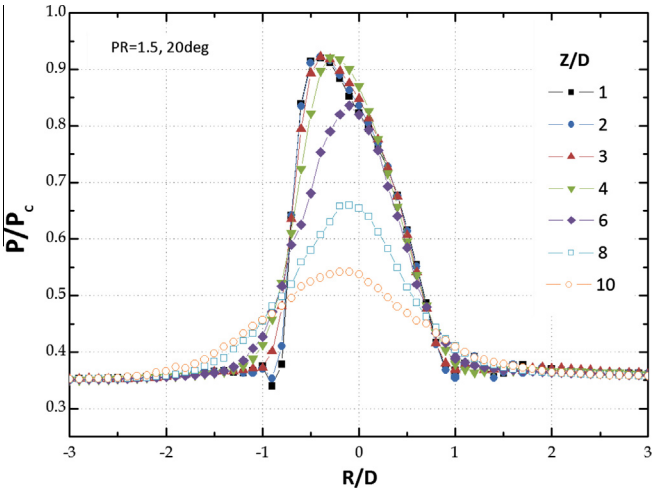

Fig. 5. Surface pressure distributions for various Z/D at 20°.

tion angle increases, the radial position where the maximum surface pressure occurs moves in the upward direction and its value becomes larger. The highest observed maximum surface pressure is about $0.94P_c$ at the 30° inclination. This phenomenon can be explained with the movement of a stagnation streamline in the upward direction as the impinged surface is inclined [9]. The stagnation pressure increases due to the small pressure loss through a weak shock wave in front of the inclined plate. When the surface is inclined to the jet flow, the plate shock in front of the surface does not form a normal shock, resulting in an increase of the maximum surface pressure. Stagnated flow in a high-pressure state is accelerated in either the upward or downward direction along the surface and the surface pressure decreases to the ambient level at ±1.0 R/D regardless of the inclination angle.

The effect of the nozzle-to-plate distance is shown in Fig. 5. In this case, the inclination angle is fixed at 20°. As the distance from the impinged surface to the nozzle exit increases, the maximum surface pressure decreases and the width of the impinged area increases due to the increase in the turbulence mixing effect. In addition, it can be seen that the position of maximum surface pressure moves closer to the center of the impinged surface for the same reason.

Fig. 6 shows IR thermal images, which are expressed as the recovery factor distribution for various surface inclination angles. As with the surface pressure review, the nozzle-to-plate distance and pressure ratio are fixed to 1D and 1.5, respectively. In the case of normal impingement, recovery factor shows the axisymmetric distributions and the low recovery factors appear around a jet stagnation region. This low recovery factor is known to appear because of the 'shock induced total temperature separation' and 'energy separation' effect in a near-wall jet flow that includes a vortex motion. For the inclined angle impingement, the difference in the cooling width between upward and downward direction of the impingement area can be observed clearly in the thermal image shown in Fig. 6. As the inclination angle increases, the low recovery factor zone becomes wider in the downward while it becomes shallower and slimmer in the upward direction region. This is due to the difference in the flow rate and speed between the two directions which cause the different phase for energy separation. The large flow rate and high flow speed strengthen the energy separation. From a comparison with the result of normal impinge-

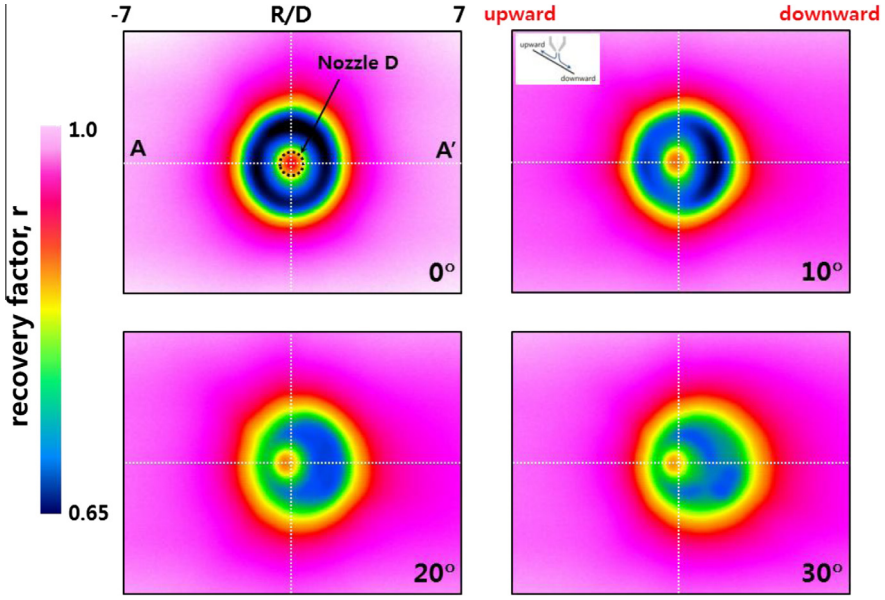

Fig. 6. Contours of recovery factor with decreasing impinging angles; exit Mach number $M_D = 1.0$, under-expansion ratio $P_e/P_a = 1.5$, nozzle pressure ratio $P_0/P_a = 2.84$, and nozzle-to-plate distance $Z_P/D = 1.0$.

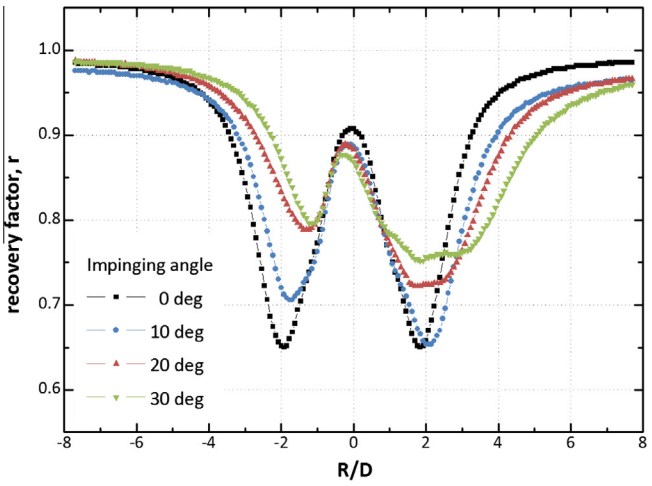

Fig. 7. Local distributions of recovery factor for various impinging angles; exit Mach number $M_D = 1.0$, under-expansion ratio $P_e/P_a = 1.5$, nozzle pressure ratio $P_0/P_a = 2.84$, and nozzle-to-plate distance $Z_P/D = 1.0$.

ment, it is found that the near wall jet cannot be cooled well in both upward and downward region when the impinged surface is inclined to the jet flow. This can be explained by the decrease in the vortex-induced energy separation effect resulting from the weakening of the secondary vortex development in the asymmetry of wall jet.

For a detailed observation, the local distributions of the recovery factor on line A–A' (in Fig. 6) are plotted for the inclination angles of 0°–30° in Fig. 7. We can see the "w"-shaped recovery factor distribution. This distribution occurs because of "energy separation" caused by the 'vortex effect' from shock-induced phenomena [2,3] and the 'imbalance' between heat conduction from the temperature difference and the viscous shear work from the velocity difference [11–13]. For the vortex effect, flows passing the secondary vortex at the impinged surface go through the adiabatic expansion, resulting in a low recovery factor on the impinged surface for close nozzle-to-plate distances plate as shown in Fig. 8. For the heat conduction and viscous shear work, fluid flow on the plate, such as air ($Pr < 1$), energy influx by viscous is smaller than both heat conduction from high velocity at the shear layer of freestream and boundary layer of the impinged plate. As a result, the low recovery factor was caused by the low energy distribution at the outside of the free jet and the inside of the boundary layer. Therefore, the downstream has a lower recovery factor than the upstream because of its high velocity at the inclined. The smaller inclined angle case has the lower recovery factor.

The peak value of the low recovery factor is appeared around $R/D = \pm 2$ in transition region ($1 < |R/D| < 2.5$, [24]) due to change of turbulence intensity [25–27]. And the cooling effect is decreased at the wall jet flow moving downstream. This means the recovery factor approached 1, as shown at the edge of Fig. 7. The low temperature region is narrower with a decrease of the inclined angle ($1 < R/D < 3$). A growth of the expansion region, due to the maximum pressure rising and moving upward appeared in Fig. 4, makes the wider cooling width. As the inclination angle increases, the minimum value of the recovery factor increases in both upward and downward region of surface.

Fig. 9 shows IR thermal images showing the recovery factor distribution for various nozzle-to-plate distances. When the impinged surface is close to the nozzle ($Z/D = 1.0$ and 2.0), the distributions are similar to each other. However, in cases of larger nozzle-

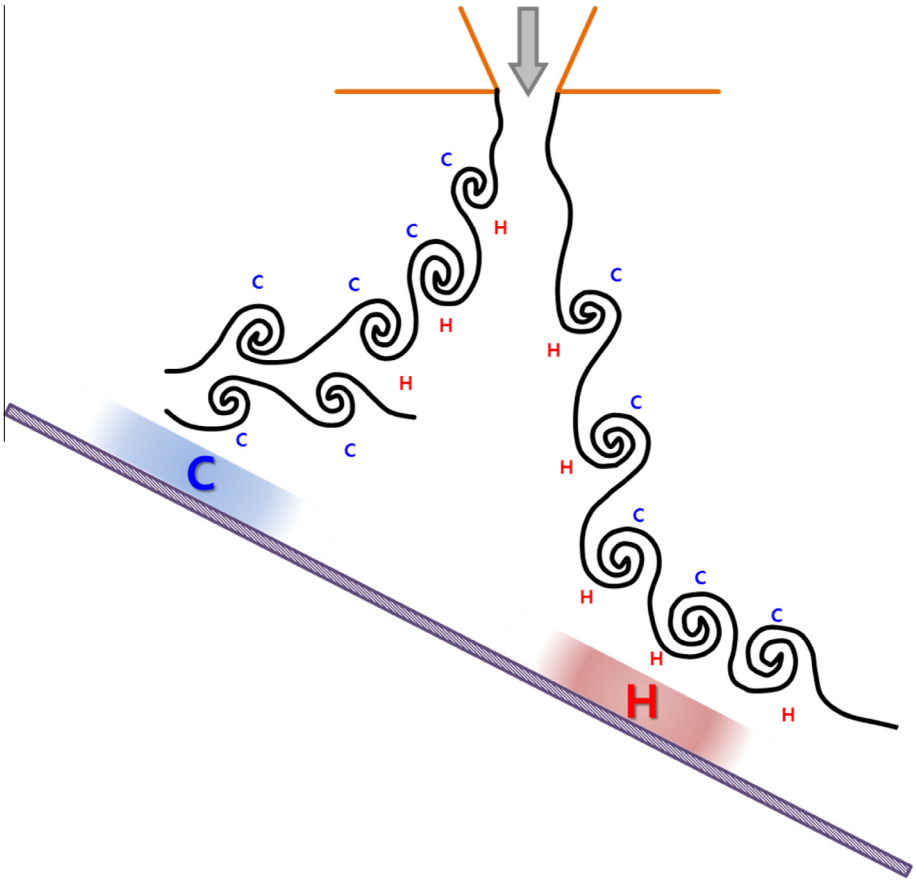

Fig. 8. Schematic of energy separation on the inclined impinging jet.

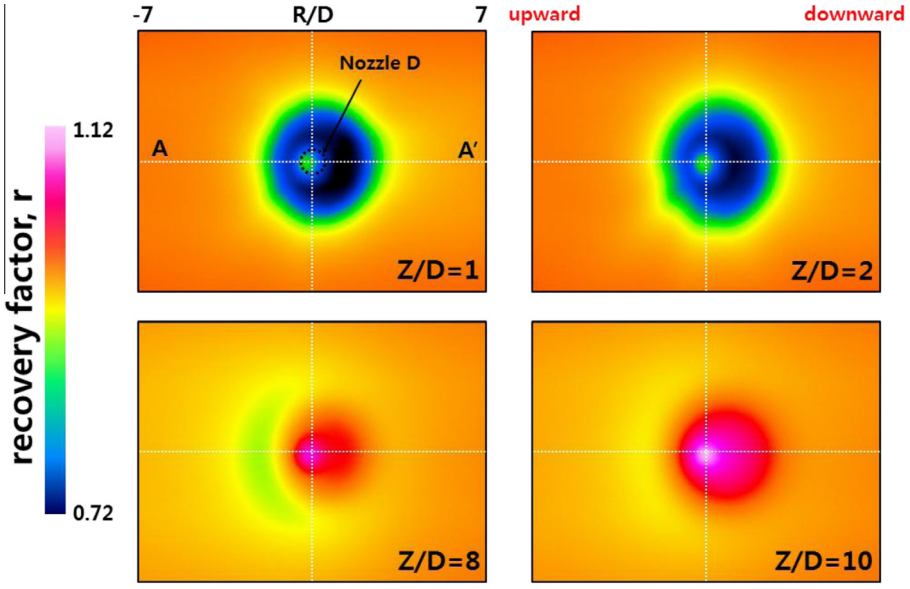

Fig. 9. Contours of recovery factor for various nozzle-to-plate distances; exit Mach number M_D = 1.0, under-expansion ratio P_e/P_a = 1.5, nozzle pressure ratio P_0/P_a = 2.84, and inclined angle 20°.

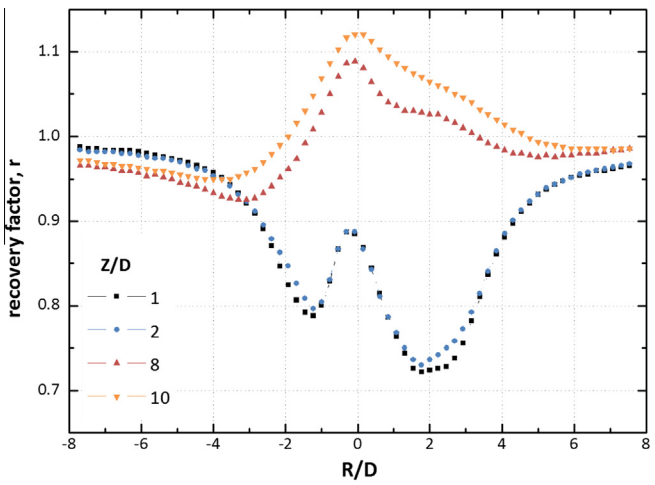

Fig. 10. Local distributions of recovery factor for various nozzle-to-plate distances; exit Mach number M_D = 1.0, under-expansion ratio P_e/P_a = 1.5, nozzle pressure ratio P_0/P_a = 2.84, and inclined angle 20°.

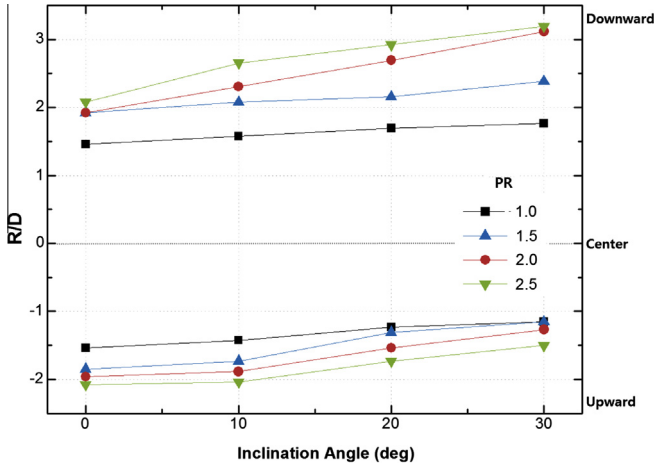

Fig. 11. Location of minimum recovery factor as functions of underexpansion ratio and impinging angle.

to-plate distances (Z/D = 8.0 and 10.0), the cooling effect nearly disappears due to the weakening of the vortex-induced energy separation effect by the secondary vortex motion on the surface. On the contrary, the heated region appears at the central and the downward direction regions of the plate. This effect has been explained by Fox et al. [2,3] as the vortex-induced energy separation effect of a primary vortex street formed around a free jet edge. It is interesting to note that the downward region is cooled more than the upward region in cases with a small nozzle-to-plate distance but is heated more than the upward region in cases with a long nozzle-to-plate distance. This is likely due to the relative large flow rate which makes increasing the energy separation at the downward direction region. It means that the hot or cold fluid particles can affect the downward region more than the upward region owing to its large amount. This phenomenon can be seen more clearly in Fig. 10, which shows the local recovery factor distribution on the line *A*–*A*' in Fig. 9. As mentioned, the downward region is affected strongly by the cooled or heated flow while the upward region still has a weakly cooled region even for the short nozzle-to-plate distances.

Fig. 11 shows locations of minimum recovery factor as functions of underexpansion ratio and impinging angle. It is note that the phenomenon of case in PR = 1.0, 2.0 and 2.5 are not presented in detail for this paper. As the pressure ratio increasing, the location of minimum recovery factor move away from the center. This is because the expansion accelerated region becomes wider toward downstream of wall jet. Then it moves the location of maximum convective speed point to downward. And the location of minimum recovery factor moves to downward with inclination angle increasing in the same pressure ratio conditions due to movement of maximum convective speed location to downward.

4. Conclusion

An experimental investigation was conducted to examine thermal characteristics of an axisymmetric, underexpanded jet impinging on an inclined flat surface. The recovery factor distribu-

tions for thermal characteristics were measured using infrared thermography.

The conclusions are summarized as follows:

1. The surface pressure measurements indicated that: as the inclination angle increases, the maximum surface pressure increases and the peak surface pressure moves upward on the plate; as the nozzle-to-plate distance increases, the maximum surface pressure decreases; when the plate is inclined, the peak surface pressure moves downward the center of the plate.
2. As the inclination angle increases, the size of cooling region on the downward region impinged surface increases in the opposite to the upward direction surface and it can be explained by the weak cooling effect resulting from a decrease of the vortex-induced energy separation effect.
3. When the impinged surface is far from the nozzle, the surface is heated by the hot gas fluid particles and the downward region is found to be affected more severely by the energy separation effect than the upward region due to the strong energy separation effect by larger flow rate impinged surface.

This study is meaningful that it provides 2-dimensional thermal characteristics data with high spatial resolution by IR thermography and shows a good IR measuring technique for the high speed impinging jet flow. The results of this study and its methodology can be used and referred to improve the thermal safety design of rocket and jet engine system applications in the future.

References

[1] K. Jambunathan, E. Lai, M.A. Moss, B.L. Button, A review of heat transfer data for single circular jet impingement, International Journal of Heat and Fluid Flow 13 (1992) 106–115.

[2] M.D. Fox, M. Kurosaka, L. Hedges, K. Hirano, The influence of vortical structures on the thermal fields of jets, Journal of Fluid Mechanics 255 (1993) 447–472.

[3] M.D. Fox, M. Kurosaka, Supersonic cooling by shock-vortex interaction, Journal of Fluid Mechanics 308 (1996) 363–379.

[4] O.I. Gubanova, V.G. Lucev, L.N. Plastina, Central breakaway zone with interaction between a supersonic under-expanded jet and a barrier, Fluid Dynamics 6 (1973) 298–301.

[5] G.T. Kalghatgi, B.L. Hunt, The occurrence of stagnation bubbles in supersonic impingement flows, The Aeronautical Quarterly 27 (1976) 169–185.

[6] I.P. Ginzburg, B.G. Semiletenko, V.S. Terpigorev, V.N. Uskov, Some singularities of supersonic under-expanded jet interaction with a plane obstacle, Journal of Engineering Physics 19 (1973) 1081–1084.

[7] J.C. Carling, B.L. Hunt, The near wall jet of a normally impinging, uniform, axisymmetric, supersonic jet, Journal of Fluid Mechanics 66 (1974) 159–176.

[8] R.J. Goldstein, A.I. Behbahani, K. Kieger Heppelmann, Streamwise distribution of the recovery factor and the local heat transfer coefficient to an impinging circular air jet, International Journal of Heat and Mass Transfer 29 (1986) 1227–1235.

[9] P.J. Lamont, B.L. Hunt, The impingement of underexpanded, axisymmetric jets on perpendicular and inclined flat plates, Journal of Fluid Mechanic 100 (1980) 471–511.

[10] K.H. Kim, K.S. Chang, Three-dimensional structure of a supersonic jet impinging on an inclined plate, Journal of Spacecraft and Rockets 31 (1994) 778–782.

[11] E.R.G. Eckert, Cross transport of energy in fluid streams, Thermo and Fluid Dynamics 21 (1987) 73–81.

[12] B. Han, R.J. Goldstein, H.G. Choi, Energy separation in shear layers, Heat and Mass Transfer 45 (2002) 47–55.

[13] B. Han, R.J. Goldstein, Instantaneous energy separation in a free jet––Part II. Total temperature measurement, International Journal of Heat and Mass Transfer 46 (2003) 3983–3990.

[14] W.S. Seol, R.J. Goldstein, Energy separation in a jet flow, Journal of Fluids Engineering 119 (1997) 74–82.

[15] D. Lytle, B.W. Webb, Air jet impingement heat transfer at low nozzle-plate spacings, International Journal of Heat and Mass Transfer 37 (1994) 1687–1697.

[16] L. Huang, M.S. El-Genk, Heat transfer of an impinging jet on a flat surface, International Journal of Heat and Mass Transfer 37 (1994) 1915–1923.

[17] T. Liu, J.P. Sullivan, Heat transfer and flow structures in an excited circular impinging jet, International Journal of Heat and Mass Transfer 39 (1996) 3695–3706.

[18] M. Behnia, S. Parneix, Prediction of heat transfer in an axisymmetric turbulent jet impinging on a flat plate, International Journal of Heat and Mass Transfer 41 (1998) 1845–1855.

[19] J.W. Baughn, S. Shimizu, Heat transfer measurements from a surface with uniform heat flux and an impinging jet, Journal of Heat Transfer 111 (1989) 1096–1098.

[20] B.G. Kim, M.S. Yu, H.H. Cho, Recovery temperature measurement of underexpanded sonic jets impinging on a flat plate, Journal of Thermophysics and Heat Transfer 17 (2003) 313–319.

[21] M.S. Yu, B.G. Kim, H.H. Cho, Heat transfer on flat surface impinged by an underexpanded sonic jet, Journal of Thermophysics and Heat Transfer 19 (2005) 448–454.

[22] S.W. Shin, B.S. Kim, J.W. Lee, M.S. Yu, H.H. Cho, Measurement of the adiabatic wall temperature in compressible high speed impinging jet, Proceedings of the Third National Congress on Fluids Engineering (2004) 623–626.

[23] B.G. Kim, Heat Transfer Measurement of Under-expanded Jet Impingement Flow on a Flat Plate, PhD Dissertation, Yonsei University, Seoul, 2002.

[24] V. Katti, S.V. Prabhu, Experimental study and theoretical analysis of local heat transfer distribution between smooth flat surface and impinging air jet from a circular pipe nozzle, International Journal of Heat and Mass Transfer 51 (2008) 4480–4495.

[25] K. Knowles, M. Myszko, Turbulence measurements in radial wall jets, Experimental Thermal and Fluid Science 17 (1998) 71–78.

[26] T.S. O'Donovan, D.B. Murray, Jet impingement heat transfer – part 1: mean and root mean square heat transfer and velocity distributions, International Journal of Heat and Mass Transfer 50 (2007) 3291–3301.

[27] D. Cooper, D.C. Jackson, B.E. Launder, G.X. Liao, Impingement jet studies for turbulence model assessment – 1. Flow field experiments, International Journal of Heat and Mass Transfer 36 (10) (1993) 2675–2684.